Matched Moving-Window Averaging Filter

*Michael E. Becker, Tobias Steinel**
Display Messtechnik&Systeme, Rottenburg am Neckar – Germany
***Instrument Systems GmbH, München – Germany**

Abstract
Some display measurement tasks with imaging light measurement devices (LMDs) require evaluation of the target quantity (e.g. luminance) exactly over the dimension of individual pixels, single lines or columns of the display under test (DUT). This can be achieved, in the case of high image sampling ratios, by application of moving window average (MWA) filtering for which we introduce a novel method of adjusting window parameters (i.e. kernel coefficients) to effectively and completely remove unwanted periodic modulations even at low sampling ratios.

Author Keywords
imaging LMD; IDMS; low-pass filtering; moving-window averaging; box filtering; convolution; stepped kernel, de-mura

1. Introduction
Ever since the first days of electronic television it has been known that imaging of periodic structures (e.g. the plaid pattern of the newsreader's jacket) in many cases is resulting in disturbing artifacts in the displayed image. Such artifacts are caused by interference between the device performing spatial sampling (e.g. electronic camera) and the periodicity of the sampled object or scene. The process causing these artifacts and distortions in static images is known as (spatial) aliasing. Well known results of spatial aliasing are "moiré" interference patterns, which are deliberately generated in special fabrics and to be controlled or avoided in the case of electronic imaging.

When imaging light-measurement-devices (LMDs) are used in the field of electronic display metrology, as specified for example in the SID Information Display Measurement Standard, IDMS [1], the regular array of display pixels is usually oversampled in the space domain (i.e. *image sampling ratios*, $R_s = 10$ ... 30 are sometimes recommended*) in order to take into account even small details of the display under test, DUT, and to reduce disturbing aliasing effects.

Some specific measurement tasks in that field require evaluation of average values of the target quantity (e.g. luminance, radiance, chromaticity) exactly over the width of individual pixels, lines or columns of the display under test, for instance, the determination of display resolution via grille luminance modulation (i.e. luminance contrast) as specified in IDMS V1.2, 7.1 and 7.2 [1] and applied in [2]. Such an adjusted averaging can be achieved, by e.g. application of moving window average (MWA, MA) low-pass filtering as detailed in section B18 of the IDMS V1.2 [1].

In the field of image processing, MWA-filtering, in the case of constant coefficients also known as "box-filtering" [3] has been used for decades for e.g. detection of features and patterns in satellite images, for calculation of local statistics in images at low computational costs and in life-sciences for correction of artefacts in simultaneous EEG-fMRI data evaluation.

* *image sampling ratio* is the number of LMD sensor pixels that are sampling one cycle of the image, as provided by the lens of the LMD, of the periodically patterned object under measurement (e.g. a display pixel matrix); it is sometimes shortened to "pixel ratio".

The dimensions of the "box" (i.e. the window) that defines the neighborhood of the currently considered image pixels are usually given by odd integer numbers of image pixels to avoid shifting of the filtered image with respect to the original. Box-filtering or moving (window) average filtering is equivalent to performing a convolution of the original image with kernels that specify the neighboring pixels and their weights which can be selected to widen the effect of operations beyond averaging [4]. Convolution of an image with a kernel in the space domain corresponds to multiplication of their respective Fourier transforms.

A necessary condition for correct results of the filtering process in electronic display metrology with imaging LMDs is the adaptation of the (usually square-shaped) window dimension to the pixel pitch of the display under measurement which turns out to be difficult for the case of low image sampling ratios. When in just that case an image of the regular array of display pixels is sampled by a second regular array of sensor/detector elements, even small mismatches of the involved array pitches may generate distinct artefacts in the resulting image data [5]. When the involved pitches are considerably different, that is, when the display pixel matrix is distinctly oversampled, sampling artifacts may be correspondingly reduced.

In practical applications however, the sampling ratio, R_s is limited, amongst others, by the number of elements of the sensor array of the imaging LMD and by the DUT area that is to be included in one measurement. With increasing dimensions of display screens and the need for a minimum of individual measurements, there are economical reasons that suggest lower sampling ratios.

Just as low sampling ratios (e.g. between 2 and 3) may cause faulty artefacts in images of periodic structures (aliasing), mismatches between the sampling ratio (usually a rational number) and the width of the averaging filter (odd integer number) may also cause erroneous results.

Especially at low image sampling ratios it would thus be advantageous if we could adapt the effective width of the window that specifies the pixels used for averaging to the periodicity of the object modulations (i.e. display pixel matrix) that shall be averaged out und thus suppressed.

A proposal for such an MWA-filter with adapted "non-integer (rational) window dimensions" was made in a paper about measurement of unwanted sparkle of electronic displays [6]. The measurements used in that paper for illustrating the performance of the introduced MWA-filter were made with rather high image sampling ratios, i.e. $R_s = 11$ and 27.2 while later research [7-14] has suggested lower sampling ratios since the frequencies relevant for visual perception of sparkle are rather not above the fundamental frequency of the modulations caused by the display pixel matrix. At low non-integer values of R_s however, suppression of the fundamental frequency of the periodic display-pixel modulation has been found to be not satisfactory as reported in [8] and analyzed in detail below.

ISSN 0097-996X/25/5601-0397-$1.00 © 2025

2. Types of filters

This contribution presents and discusses three types of moving window averaging filters: (1) box-filters, (2) filters with non-integer window-width, and (3) optimized stepped kernel filters.

2.1. Box filter

A filter for spatial averaging with constant weighting of all included image samples as illustrated in Fig. 1A is called "box-filter". The frequency response of a one dimensional box-filter with M identical coefficients, R_{MWA}, and with consideration of aliasing, according to [15], is given as:

$$R_{MWA}(f,M)=\frac{\sin(M\pi f)}{M\sin(\pi f)} \quad (1)$$

with the spatial frequency, f, in terms of cycles / LMD-pixel.

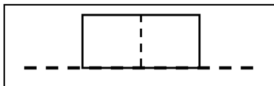

Box-filter of order $M = 2$

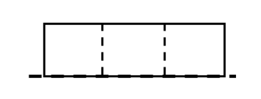

Box-filter of order $M = 3$

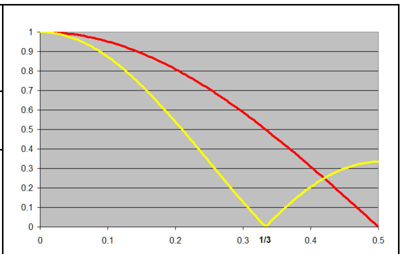

Frequency responses of box filters with order $M = 2$ (red curve) and $M = 3$ (yellow curve).

Figure 1: Box-filters of order M = 2 and M = 3 together with the respective frequency responses.

Any periodic modulation with a periodicity that is exactly an integer multiple of the image sampling ratio, R_s, can be eliminated by filtering with a window of width, $w_{MWA} = R_s$. The first zero of the frequency response of the box-filter, f_{no}, is given as $f_{no} = 1/w_{MWA} = 1/R_s$.

It should be noted, that there is no sharp separation of passed and attenuated signal frequency bands as illustrated in Fig. 1. The first side-lobe (i.e. first local maximum of transmission above the fundamental notch frequency, f_{no}) has an amplitude of 33%.

2.2. Filter with non-integer window-width

A first step toward adaptation of the filter's notch frequency to the recorded periodic modulations was presented in a paper about measurement and evaluation of unwanted sparkle of electronic displays [9]. In that specific application the modulation of the display pixel matrix has to be removed from the recorded electronic image before the sparkle contrast is calculated as the quotient of the standard deviation of random modulations that constitute the visual effect called "sparkle" and the corresponding mean value of these random modulations.

2.3. Frequency response

The actual dimensions of the kernels considered here are always positive odd integer numbers; non-integer image sampling ratios, R_s, and the corresponding "effective width", $w_{MWA\text{-}eff}$, are considered by fractional elements positioned around the core-kernel with fractions, r and r^2, originally determined by linear and bi-linear interpolation as described in [6] and illustrated in Fig. 2.

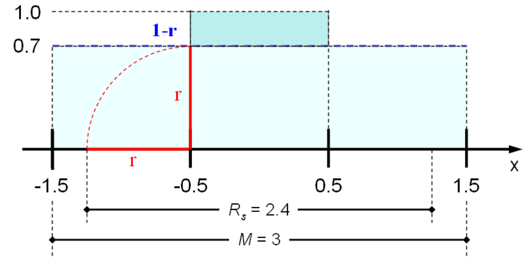

Figure 2: Construction of a 1D stepped kernel for adapting the notch frequency to the sampling ratio; for the case $R_s = 2.4$ we use a central kernel element of height 1 together with 2 side elements with height r to account for the fractional parts, i.e. $r = (2.4 – 1)/2$.

The fraction, r, according to Fig. 2 is given by:

$$r = (R_s - (\text{closest-odd-integer} \geq R_s)+2) / 2 \quad (2)$$

While a window with positive integer width, $w_{MWA} \in$ N (N: set of natural numbers), shows the first zero (notch) in frequency space at a frequency of exactly $f_{no} = 1/w_{WMA}$, this is not the case for non-integer effective widths as will be shown below.

In order to model the frequency response, $R_{MWA}(f)$, of the MWA-filter with non-integer effective window dimensions, $w_{MWA} \in \mathbf{R}$ (**R**: set of real numbers), we consider the superposition of two kernels with adjacent positive odd integer dimensions, M_i, and additional non-integer, fractional coefficients.

$$K(i,j)=\begin{bmatrix} r^2 & r & r^2 \\ r & 1 & r \\ r^2 & r & r^2 \end{bmatrix}=\begin{bmatrix} r \\ 1 \\ r \end{bmatrix}\cdot\begin{bmatrix} r \\ 1 \\ r \end{bmatrix}^T \quad (3)$$

Eqn. 3 specifies a 3x3 filter kernel, i.e. a kernel of order $M = 3$, with non-integer, fractional elements, r and r^2, at the periphery for image sampling ratios, R_s between 1 and 3. In this communication we will present a new method to determine the value of r such that the notch frequency, f_{no}, is located exactly at $f_{no} = 1/R_s$.

Since the filtering process (convolution) can be separated into

(1) filtering in a first direction, e.g. x, with $[r \ \ 1 \ \ r]$ followed by

(2) filtering in the orthogonal direction, e.g. y, with $[r \ \ 1 \ \ r]^T$,

the following considerations are presented for only one dimension (here: x) in a first step.

The order of the odd integer kernel, M, for R_s is

$$M = 2 \cdot \text{ceiling}[\ R_s/2 + 0.5\ ] – 1 \quad (4)$$

With the frequency response of a one-dimensional MWA-filter with M coefficients of 1, R_{MWA}, and with consideration of aliasing (i.e. folding of frequency components about the Nyquist frequency) according to eqn. 1 we obtain for the combination of an $M = 1$ and an $M = 3$ kernel:

$$R_{MWA}(f)=w_M\frac{\sin(M\pi f)}{M\sin(\pi f)}+w_{M-2}\frac{\sin((M-2)\pi f)}{(M-2)\sin(\pi f)} \quad (5)$$

with the weights $w_M=\frac{M r}{(M-2)+2r}$ and $w_{M-2}=\frac{(M-2)(1-r)}{(M-2)+2r}$ (6)

These weights are representing the area fractions of the kernel components as illustrated by light and dark blue rectangles in Fig. 2 under the condition $w_M + w_{M-2} = 1$.

For the parameters illustrated in Fig, 2, i.e. for $M = 3$ and r = 0.7, we obtain the weights as:

$w_1 = 0.3/2.4 = 0.125$ and $w_3 = 2.1/2.4 = 0.875$.

The frequency response of the stepped kernel according to Fig. 2 together with two box-filter responses are shown in Fig. 3.

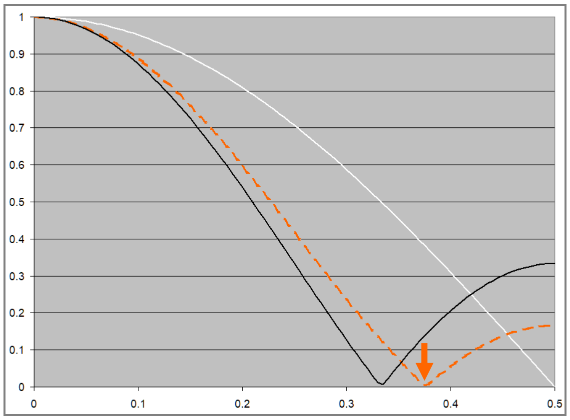

Figure 3: Frequency response of the stepped filter (orange dashed curve) according to Fig. 2 with *r* according to eqn. 2. The resulting weights are w_1 = 0.125 and w_3 = 0.875. The first minimum of the response occurs at f_{no} = 0.377 which corresponds to R_s = 2.655. The frequency responses of the box filters with *M* = 2 and *M* = 3 of Fig. 1 are shown for comparison.

It becomes obvious that a stepped filter kernel with elements determined as described above does not effectively suppress modulations with a periodicity of 2.4 LMD detector pixels as obtained by a low sampling ratio of $R_s = 2.4$.

3. Optimized stepped kernel filter

For the location of the zeroes (notches), $R_{MWA} = 0$, we obtain from (5) and (6):

$$r(f \mid M) = \frac{\sin((M-2)\pi f)}{\sin((M-2)\pi f) - \sin(M\pi f)} \tag{7}$$

with the frequency, $f = 1 / R_s$, the inverse of the image sampling ratio, R_s.

For the special case of $M = 3$ as illustrated in Fig. 2, we obtain:

$$r(f \mid 3) = \frac{\sin(\pi f)}{\sin(\pi f) - \sin(3\pi f)} \tag{8}$$

With *r* according to eqn. 6 we can calculate the effective width of the optimized MWA-window, $w_{MWA\text{-}opt}$, that suppresses periodic modulations due to e.g. the display pixel matrix with an image sampling ratio of R_s as:

$$w_{MWA-opt} = (M-2) + 2r(f \mid M) \tag{9}$$

We have calculated the frequency responses of 6 different one-dimensional filters as shown in Fig. 4. As references, the responses of two box-filters with $M = 2$ and $M = 3$ are included. For the integer width of 2.0 the response of the not-optimized and the optimized stepped kernel are identical. The box-filter with $M = 2$ has the same notch frequency as the corresponding filters with stepped kernels (both not-optimized and optimized), but the shape of the frequency response curves are quite different. The effect of the optimized kernel on the notch frequency is distinctly visible as the difference of the orange and the red curve.

The frequency response of the various kernels can also be evaluated by 2D discrete Fourier transformation of the kernels as illustrated in Fig. 5.

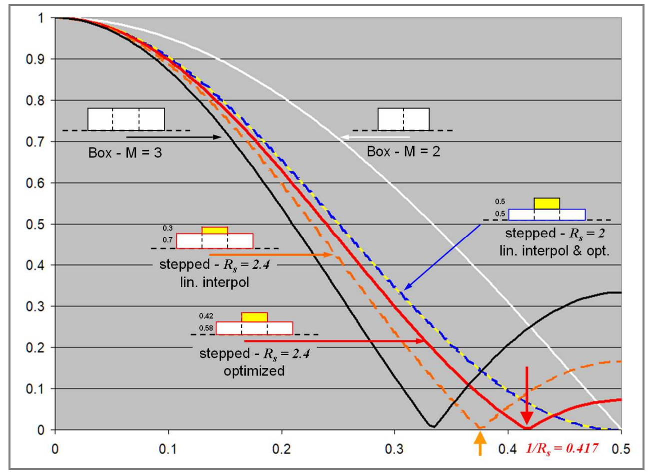

Figure 4: Frequency responses of 2 box-filters (*M* = 2 and 3, white and black curves); optimized and not-optimized stepped kernel filter for R_s = 2.0 (yellow-blue curve), not-optimized stepped kernel filter for R_s = 2.4 (dashed orange curve) and respective optimized stepped kernel filter (solid red curve).

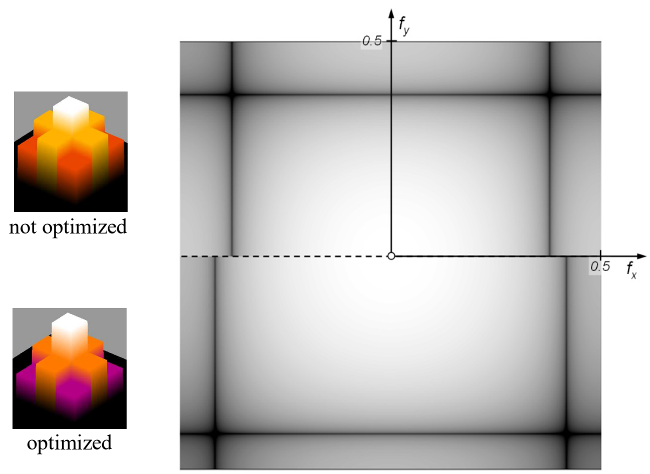

Figure 5: 2D frequency responses (log. magnitude scaling) of two 3x3-kernels with fractional coefficients at the periphery (according to eqn. 2), obtained by 2D discrete Fourier transformation of the kernels. The dark stripes parallel to x and y directions represent the frequencies that are suppressed by the filtering process (notches). The upper half of the illustration shows a notch at a frequency of f_{no} = 1/2.655 as a result of filtering with a window of width w_{MWA} = 2.4. The lower half shows the result of filtering with the optimized window width, $w_{MWA\text{-}opt}$ = 2.1547 with the notch at f_{no} = 1/2.4. The frequency is ±0.5 cycles / LMD-pixel at the edges of the diagram.

Fig. 5 illustrates the discrepancy between not-optimized and optimized 3x3 stepped kernels as obtained by 2D discrete Fourier transforms (log. magnitude) of the kernels with fractional elements at the periphery, as specified by eqn. 2. The frequency in terms of cycles / LMD-pixel is ±0.5 at the edges of the diagram in both x (horizontal) and y (vertical) direction, f_x and f_y, respectively, the origin with $fx = fy = 0$ (DC component) is in the center of the square. The dark stripes parallel to x and y directions represent the frequencies that are suppressed by the filtering process (notches). The upper half of the illustration shows a notch at a frequency of $f_{no} = 1/2.655$ as a result of filtering with a window of width $w_{MWA} = 2.4$. The lower half shows the result of filtering with the optimized effective window width, $w_{MWA} = 2.1547$ with the notch located exactly at $f_n = 1/2.4$. This mismatch illustrates the deficiency of the original method at low sampling ratios which is overcome by the introduced new method.

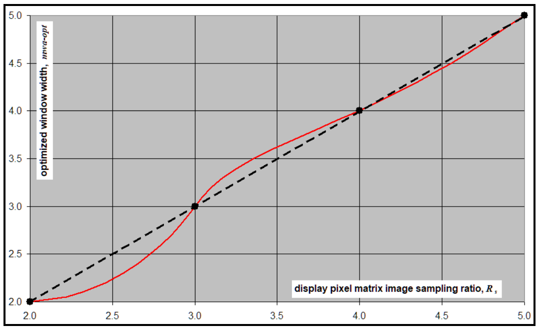

Figure 6: Optimized effective width of the moving average window, $w_{MWA\text{-}opt}$, as a function of the sampling ratio of the image of the display pixel matrix, R_s, obtained from eqns. 6 and 8. Deviations from the case $w_{MWA} = R_s$ (dashed diagonal line) are most pronounced in the range $2 < R_s < 3$. Above $R_s = 5$ the deviations are below 1% and can possibly be neglected.

Figure 6 illustrates the variation of the effective width of the optimized kernel, $w_{MWA\text{-}opt}$, with the sampling ratio, R_s, of the modulation due to the display pixel matrix.

Deviations are zero for integer values of R_s, most pronounced in the range $2 < R_s < 3$, reduced in the range $3 < R_s < 4$ and above $R_s = 5$ they are below 1% and can possibly be neglected.

4. Worked example

In order to illustrate the effect of the new filtering method, we have generated an image of a display pixel matrix with a sampling ratio, R_s, of 2.400 using the cosine-function. This ensures that no unwanted frequency components are present in the synthetic image that may disturb the evaluation.

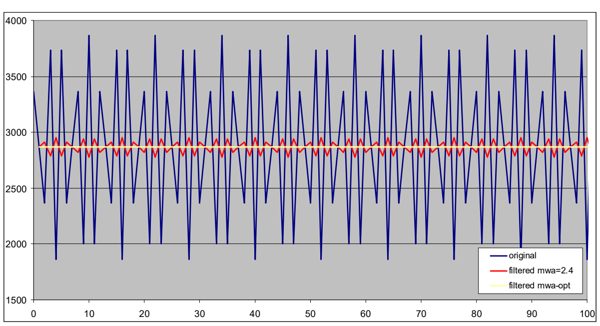

Figure 7: Intensity profile of the cosine-function sampled with $R_s = 2.4$ samples per cycle (blue curve). After filtering with a window width of 2.400 LMD-pixels (red curve) the modulation is reduced but still present. Filtering with the optimized stepped kernel filter (*mwa-opt* = 2.1547) eliminates the modulation.

	original	**2.4000**	**2.1547**
modulation	0.34891531	0.03088419	8.0966E-08
stdev / mean	24.6078%	2.1924%	**0.0000%**

Table 1: Specification of the effect of filtering according to Fig. 7

5. Impact

With the formalism described above, the effective width of the moving (window) averaging filter, w_{MWA}, can be adjusted in order to accurately suppress the frequencies corresponding to the display pixel matrix modulation, $1/R_s$, and to remove them even for sampling ratios down to 2. This new feature allows accurate averaging over display pixel dimensions without oversampling as recommended earlier [1] and thus makes the completion of the mentioned measurement tasks (e.g. display resolution from grille luminance modulations, OLED de-mura) more economic. For the case of display sparkle measurement, improved suppression of the display pixel matrix modulations means improved null-levels (i.e. the levels of pseudo-sparkle without AG-layer) and thus increased sensitivity with respect to true sparkle modulations.

6. Literature References

[1] IDMS – Information Display Measurement Standard, issued by the Society for Information Display - Definitions and Standards Committee - International Committee for Display Metrology (ICDM)

[2] Becker, Michael E.: "Measurement of Visual Resolution of Display Screens", 2017 SID Symposium Digest of Technical Papers, Paper No. 62.2 (invited)

[3] McDonnell, M.: "Box-filtering techniques", Comput. Graphics Image Process. 17(1)1981, pp.65-70

[4] Gonzalez, R., Woods. R.: "Digital Image Processing", 3rd ed., Prentice Hall, 2008

[5] Holst, Gerald C.: "Sampling, Aliasing, and Data Fidelity ..., SPIE Press Series , No 55, 1998

[6] Becker, Michael E.: "Sparkle measurement revisited: A closer look ... ", Journal of the Society for Information Display, 23,10(2015), 472- 485; doi: 10.1002/jsid.391

[7] Isshiki, Masanobu, et al.: "The optimized condition for display sparkle contrast measurement ...", SID Symposium Digest of Technical Papers. Vol. 50. No. 1. 2019

[8] Isshiki, Masanobu, et al.: "Requirements for Reliable Display Sparkle Contrast Measurement: ...." SID Symposium Digest of Technical Papers. Vol. 53. No. 1. 2022

[9] Isshiki, Masanobu, et al.: "Equivalent Conditions for Display Sparkle Contrast Measurement ... " SID Symposium Digest of Technical Papers. Vol. 54. No. 1. 2023

[10] Kurashige, Makio, et al.: "Estimation of Equivalent Conditions for Display Sparkle Measurement", Proc. IDW 2019

[11] Kurashige, Makio, et al.: "Novel Approach on Sparkle Contrast Measurement by utilizing Diffraction Blur", Proc. IDW 2020

[12] Kurashige, Makio, et al.: "Error analysis of sparkle contrast ...", Journal of the Society for Information Display, 30,9(2022), pp. 680-689; doi: 10.1002/jsid.1109

[13] Becker, Michael, E.: "10 Years of Sparkle Measurement – The Lessons Learnt", electronic displays Conference 2021, Nürnberg

[14] Ferwerda, James A., et al.: "Perception of sparkle in anti-glare display screens", Journal of the Society for Information Display, 22,2(2014), pp. 129–136, doi: 10.1002/jsid.223

[15] Smith, Steven W.: "The Scientist and Engineer's Guide to Digital Signal Processing", https://www.dspguide.com